

Whispering- Gallery Mode Silica Micro-Sensors for Temperature and Gas-Phase Concentration Measurements

Q. Ma^{*}, L. Huang^{*}, Z. Guo[†], and T. Rossmann[‡]
*Department of Mechanical and Aerospace Engineering
Rutgers University, Piscataway, New Jersey 08854*

Temperature measurement utilizing Whispering Gallery Modes (WGM) in silica microspheres is analytically and experimentally studied over a wide range of temperature, cryogenic (~110K) to above room temperatures (310K). Experimental results using a resonance wavelength shift technique show excellent sensitivity and repeatability for point temperature measurements as well as the capability for ultra-high-resolution operation. Gas phase molecular detection utilizing spectra shift of WGM is also shown for coated microspheres. Mie theory analysis is utilized to explain coating sensitivity. A demonstration experiment is realized using a hydrophilic SiO₂ nanoparticle coating on the microsphere. High measurement resolution (1ppm H₂O change) at low humidity levels (0%~10%) is seen which far exceeds previous studies based on the similar coating techniques.

I. Introduction

Dielectric resonators based on total internal reflection have become an excellent sensor development platform because of their light confinement characteristics and ultra-high quality factors. The optical resonance in such devices is typically given the name whispering gallery mode (WGM). The WGM concept was originally introduced to describe sound waves propagating close to the cylindrical wall in St. Paul's Cathedral, London,¹ where the acoustical modes were partially confined due to the suppression of the wave diffraction by the sound reflection from the curved dome walls. Moving the WGM phenomenon to the optical regime and shifting to micro-dimension systems has allowed the development of ultra-high resolution capabilities with the addition of improved packaging in optical WGM devices. Since WGM is a morphology-dependent phenomenon, the radius of the resonator determines the effective volumes and distribution of the modes. During the past two decades, optical whispering gallery modes have been realized in modern high quality dielectric resonators of many different shapes such as cylindrical,² spherical,³ toroidal,⁴ ring⁵ etc. They have drawn increasing attention due to their great potential in the application of cavity quantum electrodynamics,⁶ microlasers,^{7,8} optical filters,⁹ and miniature sensors.^{10,11}

For sensor applications, WGM devices have been employed with great success. An acceleration sensor was developed based on microsphere WGM resonator and pedestal antiresonant reflecting waveguide coupler.¹² Induced flexure-arm displacements were monitored through changes in the resonance characteristics of a spherical optical cavity coupled to the flexure. Better than 1 mg (acceleration) at 250Hz bandwidth and a noise floor of 100μg were achieved. A micro-optical force sensor based on WGM physics has also been developed.¹³ A compressive force applied to a hollow Polymethyl-methacrylate (PMMA) microsphere induces a change in both the shape and the index of refraction of the sphere leading to a shift in the spectral location of the WGM. Although the WGMs in dielectric micro resonators have been the subject of many significant scientific studies, few works can be found in the aspects of temperature

^{*} Graduate Research Assistant

[†] Associate Professor

[‡] Assistant Professor, Senior Member, AIAA

sensitivity and temperature sensor applications of WGM and gas phase chemical sensing, both of which are addressed in this paper

Sensor applications which employ the interaction of the WGM evanescent component with an ambient analyte medium can be characterized into two categories: measurement of frequency/wavelength shifts of WGM resonance due to change of effective refractive index and/or size of resonator,^{10,11,13,14,15} and measurement of the amount of resonator's quality factor spoiling¹⁶ or change of coupling efficiency.^{17,18} Current technology enables optical frequency measurement down to the level of $\Delta f/f \sim 10^{-10}$, leading to the claim of extremely high sensitivity for nanoscale detection.^{11,19} However, sensor material properties such as thermal expansion and the thermo-optic effect are susceptible to thermal fluctuations caused by either ambient temperature variation or the absorption of laser energy during laser scanning or pumping. These effects may induce appreciable resonance frequency/wavelength shifts, and thus, need to be considered in the development of resonance shift sensing techniques.

Cryogenic optical fiber sensors (COFS) operating at liquid nitrogen (LN₂) temperature levels have been used to measure temperature conditions for superconductors. A COFS with resolution ~ 0.4 K in the vicinity of room temperature and ~ 0.07 K in the vicinity of cryogenic temperatures using temperature dependent emission characteristics of an erbium-doped fiber (EDF) has been proposed.²⁰ Additionally, an optical fiber temperature sensor based on the analysis of the decay time of the fluorescence emitted by specially doped crystals bonded at the extremity of a multimode optical fiber was successful, where the excited state lifetime of the fluorescence is greatly dependent on temperature.²¹ However, this kind of sensor is not cost-effective, and the resolution is limited by the fluorescence emission intensity and the sensor has limited range.

Optical whispering-gallery mode effects in dielectric micro-resonators such as microspheres,^{22,23} microdisks,²⁴ or microrings²⁵ have been intensively investigated for the development of new biological and/or chemical sensors. The evanescent field of the WGM with a characteristic length of tens to hundreds of nanometers is sensitive to the refractive index change of the surrounding medium or to the binding of biological/chemical molecules to the resonator surface. A resonance frequency shift of the WGMs is induced when such events happen. The light-matter interaction is enhanced due to the long interaction length of the optical resonances associated with high quality factor WGMs. The high Q -factor is also correlated with narrow linewidths, which provide WGM-based sensors with high sensitivity when relying on a resonant frequency shift method of detection. Ref. 23 has demonstrated detection of protein molecules within an aqueous solution utilizing the refractive index change of the solution as measured by the shift of WGMs in silica microspheres. Ref. 25 also proved label-free single molecule detection with a micro-toroid resonator in aqueous solution, extending the technique to a dynamic range of 10^{12} in concentration. Ref. 24 demonstrated a sensor based on integrated optical microcavities which can measure a change of as little as 10^{-4} in refractive index of the surrounding medium.

This study looks to examine the ability of WGM-based microsensors to measure temperature and the *in situ* concentration of a trace gas-phase species. The temperature sensitivity of WGM in silica microspheres from cryogenic temperatures (~ 110 K) to near room temperatures (~ 310 K) is explored with experimental results matching the theoretical prediction well. Ultra-high resolution potential ($\sim 10^{-6}$ K using current available technologies) of WGM temperature measurement is discussed. A WGM gas sensing method that uses a coated silica microsphere is also explored. The coating is designed to specifically adsorb only the probed gas molecules (water vapor) and be transparent to the laser wavelength used. A theoretical analysis based on Mie theory is found to match the experiment result well where single ppm level detection of water molecules is predicted.

II. WGM Theory

In a spherical micro resonator that has radius R_0 , the light beams are confined inside by total internal reflection (TIR), i.e., the angles between beams and normal directions of the boundary satisfy Snell's law. The propagation path of the light inside the resonator can be approximated as a polygon as shown in Fig. 1a. By applying the phase matching principle to the resonance,

$$\frac{\lambda_0}{n_s} \cdot m = 2\pi R_0 \quad (1)$$

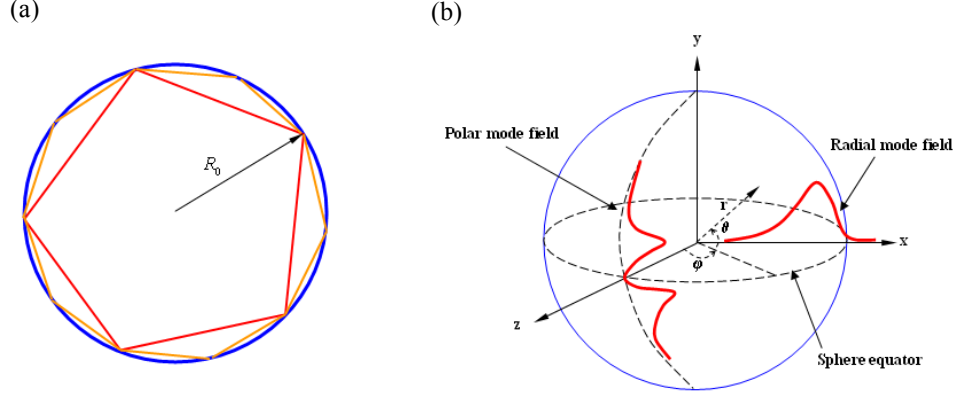


Figure 1 (a) Geometric Schematic of the WGM resonance. (b) Schematic of WGM resonance in a spherical coordinates.

where n_s is the refractive index of the micro resonator, λ_0 is the resonance wavelength and m is the azimuthal mode number. This can be used to determine the free spectra range of the WGM modes in the geometric limit.

$$FSR = \lambda_0 - \lambda_1 = \frac{\lambda_0 \lambda_1}{2\pi R_0 n_s} \approx \frac{\lambda_0^2}{2\pi R_0 n_s} \quad (2)$$

A more complete electromagnetic theory analysis in spherical systems elucidates the radial and polar mode structures (shown in Fig. 1b) as well as also gives a prediction for the resonance wavelength. As long as the resonator is significantly larger than the resonant wavelength, the difference between the geometrical and complete electromagnetic analysis is less than 1%.

The more important parameter for sensing WGM systems is the resonator quality factor (the extent of energy dissipation of a WGM mode). The Q -factor can be calculated using

$$Q = \frac{\omega_0}{\Delta\omega} = \frac{f_0}{\Delta f} \quad (3)$$

where $f_0 = \omega_0/2\pi$ and Δf are the frequency and $FWHM$ of the resonance, respectively. Figure 2 illustrates an example of the spectrum of a WGM resonance with $Q \approx 2 \times 10^7$ at a center wavelength around 1531nm showing the Lorentzian behavior of the lineshape.

The Q -factor depends on the loss mechanisms causing the optical energy to leak out of the resonator. The elements which effect the Q -factor are the scattering losses due to surface roughness, losses due to surface contamination, absorption losses due to molecular resonance, radiation losses due to boundary curvature of propagation, and loss due to energy coupling through a fiber taper. Theoretical treatments have shown that Q -factors in excess of 10^{11} are possible for microsphere resonators; however, fabrication challenges have limited the maximum achievable values to $< 10^9$.

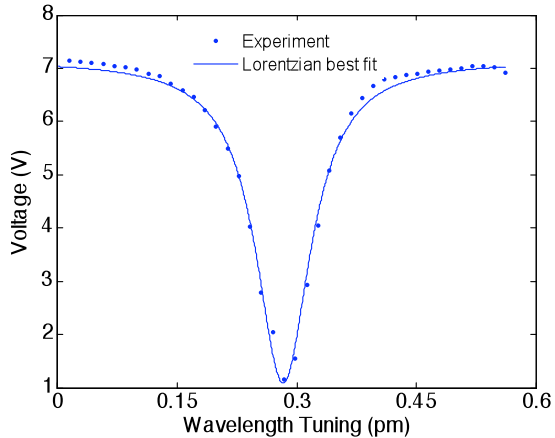


Figure 2 Spectrum of a WGM resonance at a center wavelength near 1531nm ($Q \approx 2 \times 10^7$).

III. Fabrication of Microspheres

The particulars of the fabrication techniques used in this study can be found in greater detail in Ref. 26. A short summary is provided here. A high-quality micro resonator used for the generation of high Q -factor optical whispering gallery modes is made by melting the tip of a stripped and cleaned silica optical fiber with a high power heat source (oxy-hydrogen torch). The surface tension shapes the melted material at the fiber tip into a microsphere. Using taper fibers, microspheres as small as 50 microns in

diameters are easily fabricated.

In order to utilize high Q -factor spherical optical resonators, a major challenge is to excite the whispering gallery modes efficiently without compromising the Q -factor. The modes in the optical resonator are highly confined and thus are not accessible by a free-space beam. Employment of near-field couplers are required for efficient energy transfer with fiber tapers showing the best light coupling efficiencies to the microsphere WGM. For the fabrication of the fiber taper, a computer-based programmable heat-and-pull system as well as a hydrofluoric acid etching system is built. High quality fiber tapers with sub-micron waist size and negligible tapering loss are produced by the heat-and-pull method that generates more repeatable results. Adiabatically tapered fibers with diameters from 300nm to 3 micron can be generated in this manner. A fiber polarization controller is used to optimize the coupling and to switch between TE and TM mode coupling. This allows for the optimization of the Q -factor and energy coupling for a particular microsphere/fiber taper combination.

IV. Temperature Measurement

WGM systems are ideally suited to make temperature measurements due to their small size and appreciable resonance frequency/wavelength shifts with changing temperature. In addition, these effects should be well understood to calibrate thermal drift and bias errors induced in other wavelength shift WGM techniques. We investigate the resonance wavelength shifts of fused silica microspheres with well-controlled temperature changes. The theory behind the spectral shift of WGM resonances with changing temperature is fairly simple and relies on the polygon resonator model presented earlier. For an azimuthal mode number m ,

$$k \cdot 2R \sin \frac{\pi}{k} = m \frac{\lambda}{n} \quad (4)$$

Eq. 4 represents the interference condition for the resonator. Differentiating this result and examining the temperature dependence of the index of refraction gives,

$$\frac{d\lambda}{dT} = (\alpha + \beta)\lambda \quad (5)$$

where α is the linear coefficient of thermal expansion and β is the thermo-optic coefficient of the resonator material. The temperature sensitivity should not depend on the resonator size. For silica, the thermo-optic coefficient is more than one order of magnitude larger than the thermal expansion coefficient, thus making the temperature sensing scheme largely based on the temperature dependent index of refraction of the resonator material.

Figure 3 shows the experimental setup for the WGM-based temperature measurements. The micro-bead is precisely positioned by a 3D differential translation stage (MAX302, Thorlabs) to couple with the fiber taper in the cell. The fiber taper is held by two fiber clamps. The microsphere-taper coupling is observed under a stereo-microscope (SV8, Zeiss) to place the microspheres in contact with the taper. A DFB 1531

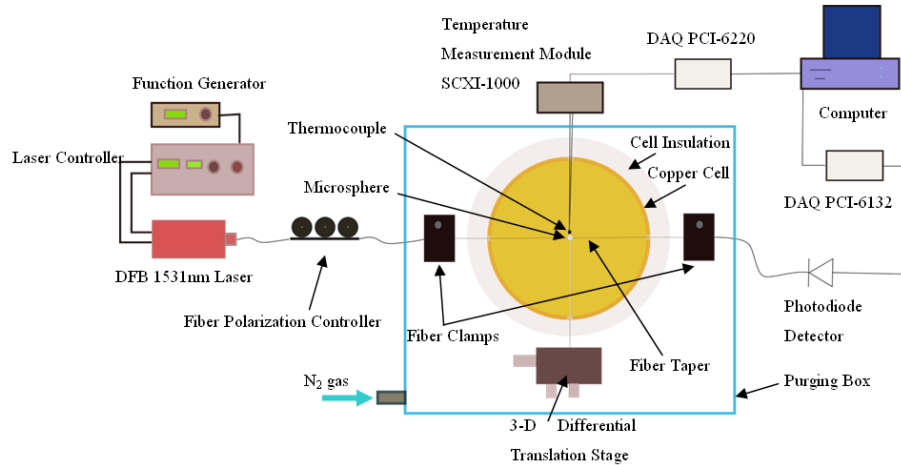


Figure 3 Experimental setup for temperature sensing experiments.

nm laser (NLK1556STG, NEL) is coupled into the fiber taper. The transmission signal is detected by a photodiode detector (PDA400, Thorlabs) and recorded by a computer equipped with DAQ cards (National Instruments). A thermocouple (Omega K-type with 0.01" bead and 0.4 s time constant) is positioned about 0.1mm away from the microsphere to monitor the temperature change around the microsphere. The temperature measured by the thermocouple is recorded simultaneously with the recording of the WGM resonance spectrum by a temperature measurement module (National Instrument). The two DAQ cards are synchronized using a Master-Slave configuration in LabView. To get high data throughput for the WGM spectra, the transmission signal is acquired at a rate of 1.25MHz, while the temperature measurement is acquired at a slower rate of 1000Hz and averaged for 0.1 sec.

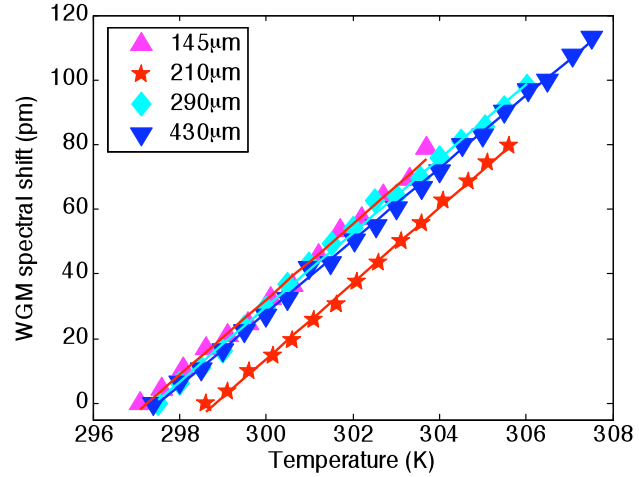


Figure 4 Experimentally measured WGM resonance wavelength shifts against temperature variation for the tested microspheres. Reprinted with permission from J. of Appl. Phys. D, 41, 245111 (2008). Copyright 2008 IOP Publishing.

The WGM microsphere is placed in a thermally controlled cell due to the influence of random thermal currents in the room air. It is observed that the wavelength shift fluctuates with an amplitude of 5 pm for the case when the sphere is placed in free air; while the fluctuation amplitude is less than 0.1 pm for the case when the sphere is placed inside the cell. These random temperature fluctuations significantly degrade the minimum temperature detectivity of the method, and thus need to be minimized. A simple thermal analysis of the system shows that the Biot number for a 400 micron silica sphere is 0.04; thus, the effects of internal temperature gradients internal are not considered. The time response of the same sphere can be calculated to be 0.8 seconds using lumped capacitance. For the smallest spheres in this study (80 microns), the thermal time constant is 0.03 seconds and the Biot number is < 0.01 .

For the spectral shift measurements, an optical spectrum analyzer (AQ6317B, ANDO) is used. A significant WGM resonance that appears in each tuning is selected for measuring the resonance wavelength shift. This WGM resonance is then tracked as the local temperature changes and a red shift is seen with increasing temperature. Microspheres with diameters of 145μm, 225μm, 290μm and 430μm, respectively, are measured for wavelength shifts versus temperature changes near room temperature (Fig. 4). The temperature sensitivity (wavelength shift per unit temperature change) for each of the tested microspheres can be best determined by linear fitting of the experimental data. The analytical temperature sensitivities of a pure silica microsphere can be calculated from Eq. 5 using the resonance wavelengths of the microspheres measured at room temperature and the values of $\alpha = 0.55 \times 10^{-6} \text{ K}^{-1}$ and $\beta = 8.52 \times 10^{-6} \text{ K}^{-1}$ for bulk silica at a wavelength of around 1531 nm and at a temperature of about 303 K.²⁷ The analytical temperature sensitivity (13.89 pm K⁻¹) is significantly different than the measured sensitivity of the tested microspheres (Table 1). There is no size effect to the temperature sensitivity of the WGM microspheres consistent with the geometric optic analysis. The measured sensitivities are all about 81%~84% of the analytical value from the literature.

Further analysis of the temperature sensing effect of WGM microspheres was performed at cryogenic temperatures to see if the sensitivity of the device continued to follow theoretical predictions. There is a need for the development of electromagnetic interference-immune high-resolution cryogenic temperature sensors. These can be employed in superconducting magnet assemblies where temperature stability and high-accuracy monitoring are critical to system operation. For the extension of our prior results to the cryogenic regime, a thermally insulated optical test cell is designed and cooled using liquid nitrogen. The details of this setup can be found in Ref. 28. To cool down the test cell, the liquid nitrogen is poured into the insulated test cell. Gaseous nitrogen purging continues during the entire experiment period to avoid frost formation on the optical system. For this study, stable temperatures in the range from 113 K to 293 K were experimentally achieved.

Table 1 Comparison of analytical and measured temperature sensitivity of silica microspheres

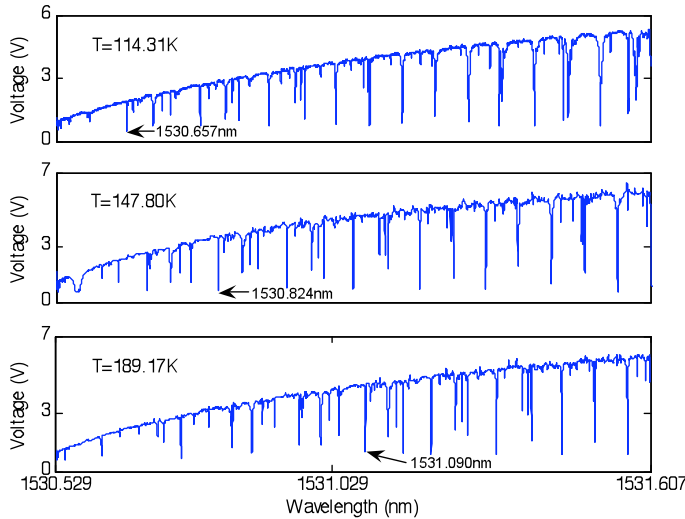
Microsphere diameter (μm)	Resonance wavelength at room temperature (nm)	Analytical sensitivity (pm/K)	Measured sensitivity (pm/K)
145	1531.978	13.90	11.42±0.51
210	1531.954	13.90	11.66±0.30
290	1531.113	13.89	11.50±0.33
430	1530.335	13.88	11.20±0.18

After optimizing the coupling with the 3D differential translation stage and the polarization controller, a significant TE WGM resonance that appears in each recorded spectrum is selected for measuring the resonance shift with respect to the temperature rise. Generally, the loaded Q -factor of the selected resonance is about 10^7 in the current study. Figure 5 shows the measured WGM spectra from a typical microsphere (225μm) at three different temperatures. Again, a significant red shift is seen as the temperature of the microsphere increases. Microspheres with diameter 85μm, 170μm, 225μm, 335μm and 435μm, respectively, are measured for their wavelength shifts versus temperature change. Although slight differences exist among the various size microspheres, no significant size effect is noted. The average sensitivity of the all the microspheres tested is shown in Fig. 6 and compared to the calculated analytical sensitivity of bulk silica. The ratio between the measured and analytical sensitivity curves is almost constant at 0.8 suggesting that the thermo-optical properties of the fabricated optical microspheres in this study is slightly different than bulk silica. Alternatively, it may indicate that the effective sum of $(\alpha+\beta)$ for the fused silica microspheres made of the Corning SMF-28e fiber is approximately 79–80% of the value for bulk Corning 7980 silica.

WGM-based temperature sensors are frequency modulated (FM) sensors and should exhibit finer measurement resolution than an intensity modulated (IM) sensor such as a thermocouple. The temperature resolution of the WGM microsphere system depends on the wavelength resolution of the readout laser/detector combination and the previously measured temperature sensitivity. The temperature resolution of a WGM sensor is formulated as

$$\Delta T_{\min} = \Delta \lambda_{\min} / (d\lambda / dT) \quad (6)$$

in which $\Delta \lambda_{\min}$ is the wavelength resolution of the instrument and $d\lambda/dT$ is the temperature sensitivity of the microsphere. The wavelength resolution is restricted by the linewidth of the scanning laser, the sampling rate in data acquisition, and the loaded WGM resonance Q -factor. The minimum resolvable resonance shift is about one-hundredth of the resonance linewidth ($\lambda/(100Q)$).¹⁹ Since the intrinsic Q -factor of a

**Figure 5 Typical transmission spectra of the microsphere 225μm in diameter at three different temperatures.**

microsphere resonator is extremely high, the loaded Q can always push to the limit of the laser linewidth. Therefore, Q -factor may not be a limiting factor and the laser linewidth, which convolves with the resonance linewidth during readout, is typically the limiting factor. Current DFB lasers have spectral linewidths in the 1MHz range, equivalent to 0.008 pm. Thus, the minimum resolvable temperature of the current instrument is 0.7 mK and 1.4 mK for temperature at 300 K and 150 K, respectively. No existing cryogenic temperature measurement devices exhibit

such a high resolution. The use of external cavity diode lasers or ring lasers that exhibit much narrower linewidths (typically 10s of kHz) would reduce the minimum temperature resolution to several micro-Kelvin.

V. Water Vapor Concentration Measurement

A potential WGM gas sensing method is explored that uses a coated silica microsphere. The coating is designed to specifically adsorb only the probed gas molecules and be transparent to the laser wavelength used. The concept of coated microsphere gas sensing is illustrated in Fig. 7. The refractive index of the coating changes as it adsorbs gas molecules at different concentration levels which induces a resonance frequency shift of the WGM. The complexity of resonant absorption spectroscopy is avoided in this kind of method as the WGM resonances can be read using any laser frequency, as it is not required to be resonant with an optical transition associated with the molecule of interest. Furthermore, the measurement sensitivity is determined both by the size of the wavelength shift that can be resolved by the WGM peak and the sensitivity of the coating to the analyte species.

We have designed and fabricated an optical resonator that is coated with many nanostructured layers of SiO_2 nanoparticles to study the response of the WGM spectral shift to water vapor concentration. The most prominent merit of SiO_2 as a humidity sensing material is its compatibility with the current microelectronics industry. The response and recovery times of the SiO_2 films are as short as milliseconds, making them well suited to performing time resolved measurements.²⁹ However, most prior works have demonstrated reliable detection of water vapor concentration in excess of 20%³⁰ relative humidity (RH) at atmospheric pressure and room temperature. For example, a recently demonstrated humidity sensor based on a long-period fiber grating coated with a thin film of SiO_2 nanoparticles can measure a RH range of 20% to 80%.³¹ For the long period fiber grating device described in that work, the minimum humidity detectivity was determined to be on the order of 1% RH. In our study, utilizing a similar hydrophilic coating applied to a microsphere resonator, the WGM spectral shift response to water vapor concentration from 0% to 10% RH was measured to far exceed the previous minimum detectivity reported for a nanostructured SiO_2 coating.

For coated microspheres, a theoretical treatment of the resonant modes in the active coating is useful for determining the sensitivity of the WGM gas sensor. The radial distribution of WGMs in a coated microsphere can be described by Mie theory and the modes are shown in Fig. 8 for the conditions of the coating used in this study. The refractive index of the microsphere is greater than the initial refractive index of the SiO_2 nanostructured coating, approximately $n = 1.22$ and increasing with absorbed water vapor. The coating thickness is 330nm. Due to the small energy fraction in the coating ($< 1\%$ of total energy in the microsphere), this method is expected to have moderate index of refraction sensitivity (3.6 nm/RIU, where RIU is a refractive index unit).

In order to fabricate the SiO_2 nanoparticle-based film, we adopted the technique of electrostatic self-assembly

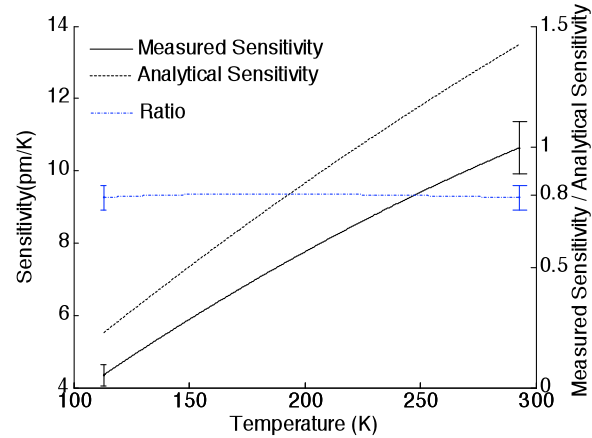


Figure 6 Comparison of the measured sensitivity with the analytical sensitivity based on the properties of bulk Corning 7980 silica, and the ratio profile of the measured sensitivity to the analytical value in the test temperature range. Reprinted with permission from Meas. Sci. Tech., 21, 025310 (2010). Copyright 2010 IOP Publishing.

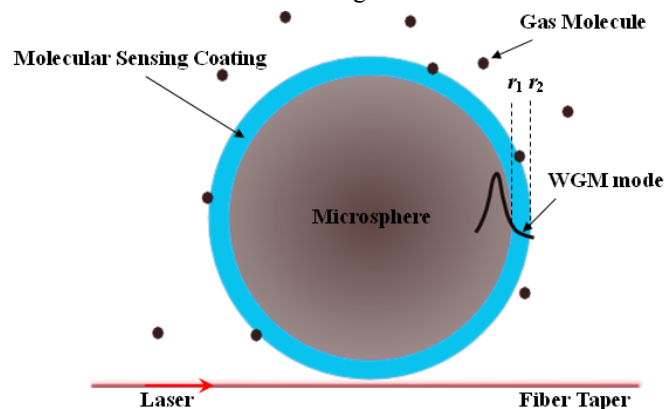


Figure 7 Illustration of the WGM gas sensing with coated microsphere.

(ESA), which has the advantages of both self-assembly and molecular control of the structure of the coating, molecular layer by molecular layer. Other researchers have used this type of coating previously and details on its fabrication can be found in Ref. 29. Figure 9 shows an atomic force microscopy (AFM) image of the surface morphology of the nanostructured coating on the microsphere. The high surface porosity and roughness enhance the behavior of the film to the super-hydrophilic regime. The contact angle of this film as fabricated onto a glass slide is measured to be less than 5 degrees, which indicates the super-hydrophilic property of the coated surface.

Following fabrication, the coated microsphere is positioned in contact with a fiber taper inside a vacuum chamber as shown in Fig. 10. A commercial relative humidity (RH) sensor (Omega OM-DVTH) with a 10s time constant and a resolution of 0.01%RH is placed near the microsphere to measure and record humidity changes inside the chamber. Nitrogen purging for several hours is used to decrease the humidity in the vacuum chamber to near 0% (within the accuracy $\pm 2\%$ RH of the commercial RH sensor). A water vapor source (wet cotton stick) is then inserted into the chamber through another port to increase the humidity in the chamber in a controlled manner through evaporation. Laser light from a tunable DFB laser diode (1653nm) is coupled into the coated microsphere for WGM by evanescent coupling from the adiabatic fiber taper. The tunable laser repeatedly scans across a wavelength range of approximately 170pm using sawtooth current modulation to resolve the spectral location of the WGM as a function of the changing environmental parameters. The WGM spectral positions are recorded at the output end of the fiber taper by detection of the transmitted light intensity as a function of time, which is then temporally correlated with the wavelength modulation of the laser.

As the humidity of the chamber decreases, the water desorbs from the pre-hydrated nano-structured silica film, causing the effective refractive index of the coated layers to decrease, hence blue-shifting the WGM resonance wavelength. Once the chamber humidity reaches the minimum value, the water vapor source increases the humidity and the water begins to be adsorbed by the nano-structured silica film, starting from sub-monolayer coverage and progressing to physisorption of bulk water into the film. As the water occupies the nanoporous network, the effective refractive index is increased, while the resonance of the WGM shifts to larger wavelengths. The temperature inside the chamber is maintained at 298.2 ± 0.1 K during the test, as measured by the commercial sensor (0.01K resolution).

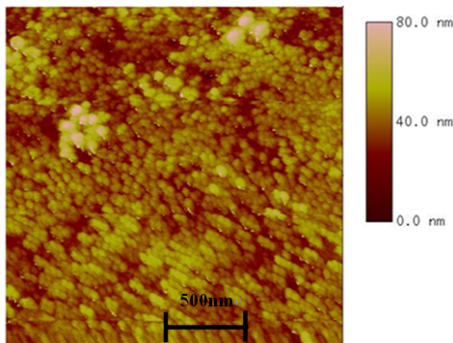


Figure 9 AFM image of the ESA SiO_2 film composed by 20 monolayers of 20nm nanoparticles.

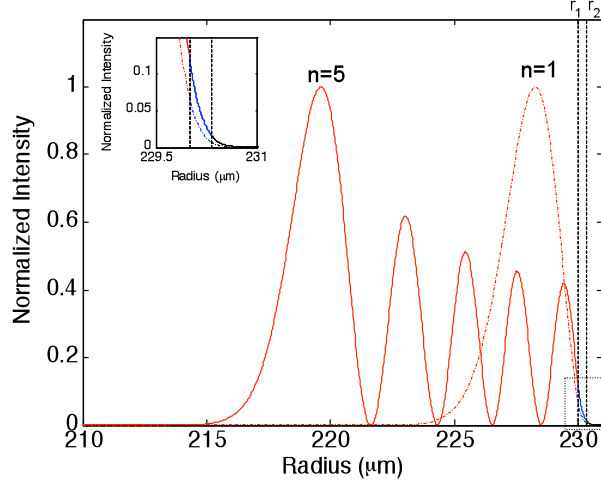


Figure 8 Intensity distribution of two TE WGMs ($n=1$, $l=1264$, dashed and $n=5$, $l=1216$, solid) with $r_1=230\mu\text{m}$ and $r_2=230.33\mu\text{m}$. Dashed lines show the boundaries of the 330nm thick coating. Refractive indices: $n_1=1.4862$, $n_2=1.22$, $n_3=1.0$. The inset shows the evanescent tail of the two radial modes in more detail.

To obtain the WGM temperature sensitivity of this coated microsphere during the humidity test, the RH is kept at a constant of 5% and the spectral shift is measured against a temperature change of 297.7K to 298.7K in the chamber. The sensitivity to temperature changes is 13.2 ± 0.01 pm/K, showing that the thin coating does not significantly affect the overall temperature sensitivity of the micro-resonator. The spectral shift of a randomly selected, strongly coupled WGM versus RH is shown in Figure 11, corrected for any temperature variations during the test. The WGM spectral shift is approximately 16pm during the humidity loading phase and 18pm during the humidity unloading phase of the experiment, which corresponds to refractive index changes of 0.0046 and 0.0052 RIU,

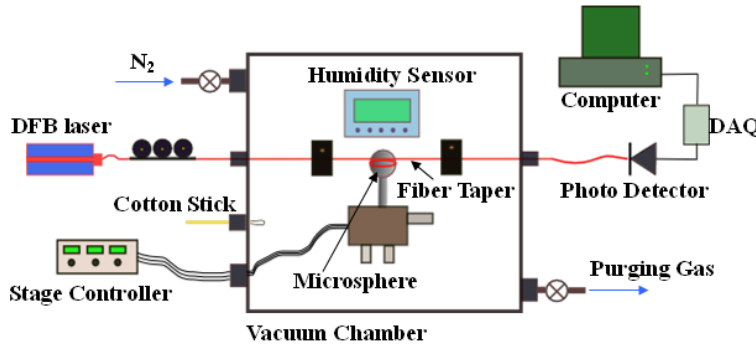


Figure 10 Experimental setup for the very low humidity (0%~10%) sensing.

this study is 0.8×10^6 . From prior experience, a shift of 1/100 of the related linewidth can be easily resolved by the detection scheme employed, which correlates to a spectral shift sensitivity in the range of ~ 0.02 pm. Using the sensor responsivity at very low humidity (0.02 pm/ppm H_2O) to estimate the minimum detectivity, a change of 1 ppm H_2O (0.003 %RH) should be resolvable using this coated WGM microspheres. Finer resolution could be achieved if such a coated microsphere is fabricated with a higher Q -factor; however, limitations in our fabrication process typically limit the maximum achievable intrinsic Q value to less than 10^9 . The coated microsphere geometry represents a significant enhancement of low humidity detection when compared to long period fiber grating methods that employ similar coatings. In addition, we can see that the coating behaves similarly in the spherical geometry for the microsphere and the cylindrical geometry for the fiber optic sensors as the humidity sensitivity of the coating is measured to be 5.8×10^{-6} RIU/ppm H_2O in this study as compared to the range of $3 \times 10^{-6} \sim 8 \times 10^{-6}$ RIU/ppm H_2O as demonstrated by Ref. 31.

Significant hysteresis phenomenon is present in Fig. 11, which may be due to finite rate effects in the SiO_2 coating. Insufficient information about the specifics of the water vapor adsorption and desorption to the particular nanoporous coating used in this study is available to generate a theory as to why the directionality of humidity change causes differing values of sensitivity. This behavior is not the result of temperature shifts in the vacuum chamber as the data has been corrected for any slight changes in environmental temperature during the experimental. In addition, it is likely not do to water vapor concentration gradients in the test chamber as the experiment was conducted with very slow humidity variation (0.02% per minute, maximum), allowing sufficient time for diffusion. Further tests on the time response of the coating are necessary to determine the finite rate effects on water vapor sensitivity.

VI. Conclusions

This paper has addressed the measurement of temperature and water vapor concentration using WGM-based microsphere resonators using the spectral shift of the resonance modes in response to changes in the external environment. To measure the temperature sensitivity of WGMs in a range from approximately 110K to 310K, a temperature controlled optical test cell for enclosing WGM coupling system was built. The measured WGM temperature sensitivity matches with the theoretical prediction well, however there is some discrepancy due to the lack of knowledge of optical fiber temperature dependant optical and mechanical properties. Ultra-high resolution temperature measurement was discussed by comparing the resonance linewidth and temperature sensitivity of the WGM resonance frequency shift. The potential

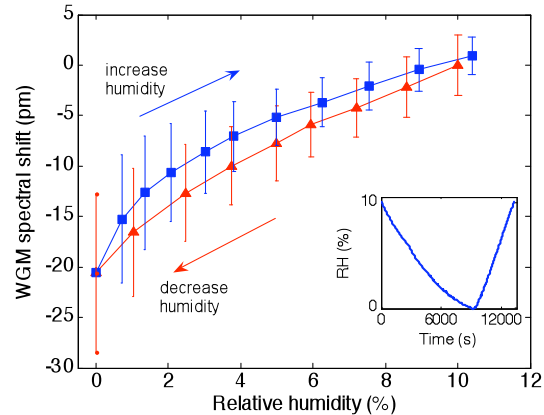


Figure 11 WGM spectral shift versus relative humidity change at 298.2K, inset: humidity change versus time.

for micro-Kelvin measurement resolution was predicted using improved WGM coupling systems and narrow linewidth lasers. Cryogenic applications of the sensor were also addressed.

For humidity sensing and water vapor detection, a microsphere coated with SiO₂ nanoparticles using an electrostatic self-assembly approach was used for a study of WGM spectral response to water vapor adsorption and desorption. The humidity was well controlled at low ambient levels (0~10%) for the tests in a specialized chamber. The resulting WGM water vapor sensitivity matches well with a theoretical analysis based on Mie theory for a coated microsphere. A change of 1ppm water molecule is found to be resolvable from the spectral shift using the current optical setup.

Acknowledgments

The authors would like to thank Prof. D. Denhardt in the Department of Biology and Prof. Q. Huang in the Department of Food Science at Rutgers University for their support with the humidity coating development and atomic force microscopy work, respectively. This research is sponsored by the US National Science foundation under grant CBET-0651737, the US Department of Agriculture CSREES Award 2008-01336, and the Rutgers University Academic Excellence Fund.

References

- ¹ Rayleigh, J.W.S., *The Theory of Sound*, Vol. II, Dover, New York, 1945.
- ² Balistreri, M. L. M., Klunder, D. J. W., Blom, F. C., Driessen, A. and Hoekstra, H. W. J. M., Korterik, J. P., Kuipers, L., and Hulst, N. F., "Visualizing the whispering gallery modes in a cylindrical optical microcavity," *Opt. Lett.*, Vol. 24, 1999, pp.1829-1831.
- ³ Braginsky, V. B., Gorodetsky, M. L., and Ilchenko, V. S., "Quality-factor and nonlinear properties of optical whispering-gallery modes," *Phys. Lett. A*, Vol. 137, 1989, pp. 393-396.
- ⁴ Armani, D. K., Kippenberg, T. J., Spillane, S. M., and Vahala, K. J., "Ultra-high-Q toroid microcavity on a chip," *Nature*, Vol. 421, 2003, pp. 925-928.
- ⁵ Little, B. E., Foresi, J. S., Steinmeyer, G., Thoen, E. R., Chu, S. T., Haus, H. A., Ippen, E. P., Kimerling, L. C. and Greene, W., "Ultra-compact Si-SiO₂ microring resonator optical channel dropping filters," *IEEE Phot. Tech. Lett.*, Vol. 10, 1998, pp. 549-551.
- ⁶ Vernooy, D. W., Furusawa, A., Georgiades, N. Ph., Ilchenko, V. S., and Kimble, H. J., "Cavity QED with high-Q whispering gallery modes," *Phys. Rev. A*, Vol. 57, 1998, pp. R2292-R2296.
- ⁷ Sandoghdar, V., Treussart, F., Hare, J., Lefevre-Seguin, V., Raimond, J.-M., and Haroche, S., "Very low threshold whispering-gallery-mode microsphere laser," *Phys. Rev. A*, Vol. 54, 1996, pp.R1777-R1780.
- ⁸ Cai, M., Painter, O., Vahala, K. J. and Sercel, P. C., "Fiber-coupled microsphere laser," *Opt. Lett.*, Vol. 25, 2000, pp.1430-1432.
- ⁹ Rabiei, P., Steier, W. H., Zhang, C., and Dalton, L. R., "Polymer micro-ring filters and modulators," *J. Lightw. Tech.*, Vol. 20, 2002, pp. 1968-1975.
- ¹⁰ Arnold, S., Khoshshima, M., Teraoka, I., Holler, S. and Vollmer, F., "Shift of whispering-gallery modes in microspheres by protein adsorption," *Opt. Lett.*, Vol. 28, 2003, pp. 272-274.
- ¹¹ Quan, H. and Guo, Z., "Simulation of single transparent molecule interaction with an optical microcavity," *Nanotechnology*, Vol. 18, 2007, 375702 (5pp).
- ¹² Laine, J. P., Tapalian, C., Little, B. and Haus, H., "Acceleration sensor based on high-Q optical microsphere resonator and pedestal antiresonant reflecting waveguide coupler," *Sens. Actuators. A*, Vol. 93, 2001, pp. 1-7.
- ¹³ Ioppolo, T., Kozhevnikov, M., Stepaniuk, V., Ötügen, M. and Sheverev, V., "Micro-optical force sensor concept based on whispering gallery mode resonators," *Appl. Opt.*, Vol. 47, 2008, pp. 3009-3014.
- ¹⁴ Quan, H. and Guo, Z., "Simulation of whispering gallery- mode resonance shifts for optical miniature biosensors," *J. Quant. Spectrosc. Radiat. Transfer*, Vol. 93, 2005, pp. 231-243.
- ¹⁵ Nguyen, N. Q. and Gupta, N., "Analysis of an encapsulated whispering gallery mode micro-optical sensor," *Appl. Phys. B*, Vol. 96, 2009, pp.793-801.

- ¹⁶ Armani, A. and Vahala, K., "Heavy water detection using ultra-high-Q microcavities," *Opt. Lett.*, Vol. 31, 2006, pp.1896–1898.
- ¹⁷ Farca1, G., Shopova, S. I. and Rosenberger, A. T., "Cavity-enhanced laser absorption spectroscopy using microresonator whispering-gallery modes," *Opt. Express*, Vol. 15, 2007, pp. 17443-17448.
- ¹⁸ Guo, Z., Quan, H. and Pau, S., "Near-field gap effects on small microcavity whispering-gallery mode resonators," *J. Phys. D: Appl. Phys.*, Vol. 39, 2006, pp. 5133-5136.
- ¹⁹ Vollmer, F. and Arnold, S., "Whispering-gallery-mode biosensing: label-free detection down to single molecules," *Nat. Methods*, Vol. 5, 2008, pp. 591-596.
- ²⁰ Lee, Y. and Lee, B., "High resolution cryogenic optical fiber sensor system using erbium-doped fiber," *Sens. Actuators A*, Vol. 96, 2002, pp. 25–27.
- ²¹ Bertrand, S., Jalocha, A., Tribillon, G., Bouazaoui, M. and Rouhet, J., "Optical fibre temperature sensor in the cryogenic range," *Opt. Laser Technol.*, Vol. 28, 1996, pp. 363–366.
- ²² Ma, Q., Rossmann, T. and Guo, Z., "Temperature sensitivity of silica micro-resonators," *J. Phys. D: Appl. Phys.*, Vol. 41, 2008, 245111.
- ²³ Vollmer, F., Arnold, S., Braun, D., Teraoka, I. and Libchaber, A., "Multiplexed DNA quantification by spectroscopic shift of two microsphere cavities," *Biophys. J.*, Vol. 85, 2003, pp. 1974-1979.
- ²⁴ Krioukov, E., Klunder, D., Driessen, A., Greve, J. and Otto, C., "Sensor based on an integrated optical microcavity," *Opt. Lett.*, Vol. 27, 2002, pp. 512-514.
- ²⁵ Armani, A., Kulkarni, R., Fraser, S., Flagan, R. and Vahala, K., "Label-free, single-molecule detection with optical microcavities," *Science*, Vol. 317, 2007, pp. 783-787.
- ²⁶ Ma, Q., Rossmann, T., Guo, Z., "Fabrication, characterization and microsensing of whispering-gallery mode micro-coupling system" ASME International Mechanical Engineering Congress & Exposition, Boston, MA, Paper No.IMECE-66946, October 31~November 6 2008.
- ²⁷ Leviton, D. and Frey, B., "Temperature-dependent absolute refractive index measurements of synthetic fused silica," *Proc. SPIE*, Vol. 6273, 2006, 62732K.
- ²⁸ Ma, Q., Rossmann, T., Guo, Z., "Whispering-gallery mode silica microsensors for cryogenic to room temperature measurement," *Meas. Sci. Tech.*, Vol. 21, 2010, 025310 (7pp).
- ²⁹ Corres, J., Matias, I., Hernaez, M., Bravo, J. and Arregui, F., "Optical fiber humidity sensors using nanostructured coatings of SiO₂ nanoparticles," *IEEE Sens. J.*, Vol. 8, 2008, pp. 281-285.
- ³⁰ Chen, Z. and Lu, C., "Humidity sensors: a review of materials and mechanisms," *Sens. Lett.*, Vol. 3, 2005, pp. 274-295.
- ³¹ Viegas, D., Goicoechea, J., Corres, J., Santos, J., Ferreira, L., Araujo, F. and Matias, I., "A fibre optic humidity sensor based on a long-period fibre grating coated with a thin film of SiO₂ nanospheres," *Meas. Sci. Technol.*, Vol. 20, 2009, 034002.